Poro Hypo Plastic analysis of the progressive excavation of the Mol URL connecting Gallery

J. Desrues, P. Bésuelle, C. Coll
Laboratoire 3S, Grenoble, France
F. Collin
GEOMAC Department, FNRS - Liège University
X.L. Li
EURIDICE, SCK.CEN, Belgian Nuclear Research Center, Belgium

ABSTRACT: In the framework of a Euratom research program devoted to Nuclear Waste deposition security assessment, a numerical simulation of the excavation of a gallery in the Boom Clay layer at Mol (Belgium) has been performed In order to model the progressive excavation and lining installation process, a special sequence of desactivation/activation of sets of elements was elaborated. In particular, this numerical strategy allowed to take into account the fact that, due to the deformation of the massif as the excavation progresses, the material to be excavated once the front has reached a given position into the rock mass cannot be defined a priori, but is resulting of the modelling of the previous phases up to the present one.

1 INTRODUCTION

In the framework of the European Project SELFRAC (5th PRCD), a numerical modelling of the excavation of a gallery in the Boom Clay layer at Mol (Belgium) was undertaken. The new gallery was made to connect an existing gallery to a new shaft in the Underground Research Laboratory (URL) HADES. The finite element code used was the code Lagamine developed in the University of Liège. One of the objective of the modelling was to compare the strain localization prediction with the observations made during the excavation. The simulation was supposed to follow as closely as possible the real excavation process that took place in the URL Hades in February 2002. In particular, the geometry and the operation of the tunneling machine, the shield and the lining placement method were taken in consideration carefully. A fully coupled hydromechanical formulation was used.The constitutive model used was the hypoplastic model called CLoE developed in Laboratoire 3S in Grenoble. The material parameters used were resulting of the laboratory tests performed in the framework of the same research project.

2 DEFINITION OF THE FIELD PROBLEM

This numerical simulation concerns the excavation of the 90m length connecting gallery from the second shaft of the underground laboratory toward the initial test drift, and more specifically the prediction of the stresses, pore pressure and displacement fields around the gallery. The first shaft and the test drift have been constructed between 1980 and 1987 and have a 223m depth and 67m length, respectively (figure 1a). The construction of the second shaft started during summer 1997 and finished during spring 1999. The connecting gallery started in 2001. The test drift has been excavated manually at a mean rate of 2-3m/day while the connecting gallery has been excavated by a semi-mechanised technique at a mean rate of 2m/day. A set of instrumentation was placed from the test drift front and around the future connecting gallery in order the measure the changes of displacements and pore pressure during the excavation of the gallery. The instrumentation installed from the test drift was organised on four lines (figure 1b). The line A was placed in the test drift axis and lines B, C and D were inclined. The connecting gallery was excavated under the protection of a shield (2.405m diameter and 2.3m length) and a concrete lining (rings of 2.400m ±1cm diameter and 1m length) was placed to support the gallery. The distance between the last placed ring and the rear of the shield oscillated between 0.2m and 1.2m. The gap between the shield diameter and lining diameter induced a convergence of the clay of about 9 cm on the diameter of the hole in clay (*see remark in § 3.1*).

3 MODEL DESCRIPTION

Simulation is are performed using the FEM code *Lagamine* (Charlier 1987) developed at the laboratory *Geomac* in Liege (Belgium), with the constitu-

tive model CLoE (Chambon et al. 1994) developed at the laboratory 3S in Grenoble (France).

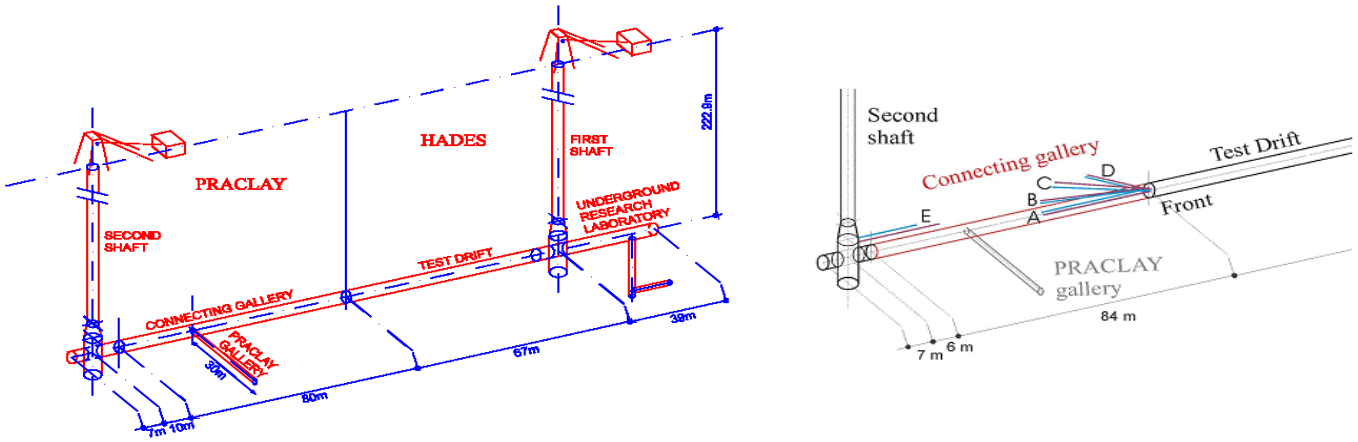

Figure 1. (a) scheme of the underground laboratory. The connecting gallery links the second shaft to the initial test drift. (b) a set of instrumentation has been placed from the test drift front and before the excavation of the connecting gallery to measure the effects of excavation on displacements and pore pressures

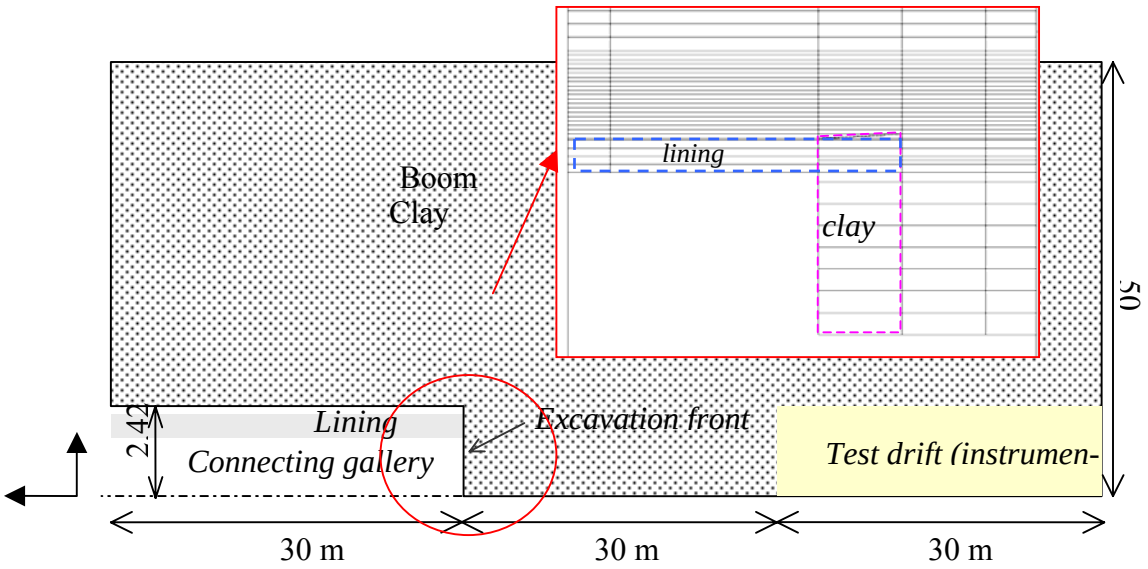

Figure 2. Geometry of the modelling zone and detail of the mesh at the excavation front, showing the superposed lining and clay blocks of elements

3.1 *Hypotheses*

The following main hypotheses have been considered:

- 2D Axisymmetric conditions along the gallery axis
- Isotropic and homogeneous initial in situ stress and pore pressure state: variation with depth is neglected in the modelling zone
- The shafts are not considered
- The unilateral nature of the contact between the clay and the lining is modelled
- The excavation is supposed to be undrained, that is to say no water can flow through the boundaries
- *Remark* : In the simulation, the gap was set to 4 cm on the diameter, for consistency with the blind prediction input data of the CLIPEX project (Bernier et al. 2002).

3.2 *Geometry*

The modelling zone is corresponding to the region around the gallery and the head of the Test Drift (instrumented zone in the CLIPEX project). The modelling domain is 50 meters high (the gallery radius is 2.00 meters) and 90 meters long. The height excavated is 2.42 meters and the thickness of the concrete lining is 0.40 meter. The initial gap between the soil and the lining is 2 cm large.

The mesh is composed of 8095 nodes and 2768 elements. The density of mesh is maximal near the roof of the gallery and relatively high in the instrumented zone (Figure 1). A set of elements, meant at modelling the lining, is defined in the mesh, placed in the final position of the lining along the gallery after excavation. These elements have the mechanical properties representative of the lining (a concrete tube with young modulus = 15 GPa and Poisson Coefficient = 0.3), but they are activated only in due time in the modelling process. Before the activation,

the elements do not play any role. The activation process is made by sub-sets corresponding to an excavation step.

3.3 *Modelling procedure*

Boom Clay is considered as a porous medium subjected to hydro-mechanical coupling (Collin et al 2002). Two major stages are included in the modelling procedure of the excavation :
Stage 1: *stress release in the first 30 meters of the connecting gallery, starting from the second shaft, in 15 days).* This step consists in decreasing the total stress on the tunnel wall from the in-situ stress down to zero. In the initial state for this stage, the concrete lining is already activated in the 30 meters zone but the soil is not in contact with it. During the release of the stress, the soil moves (it converges towards the decompressed zone) and progressively the initial gap (2 centimeters) disappears. Technically, the contact between the soil and the lining is modelled by using special elements namely *contact elements* (Cescotto & Charlier 1993), and foundation elements, inserted between the rock and the lining, and sharing their nodes with the latter. The contact elements allow to define a contact pressure. A *penetration distance* is defined at the contact zone because the contact elements are not perfectly rigid. The foundation elements transfers the stresses to the lining.

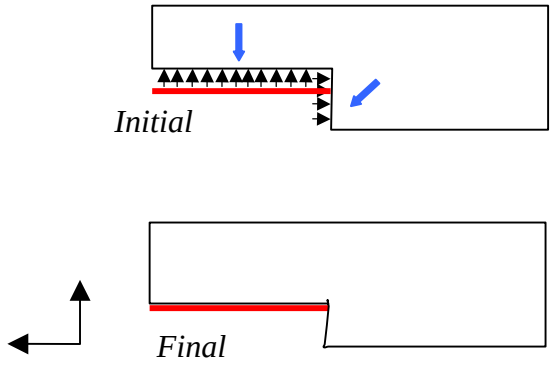

Figure 3: Stress release in the gallery

Stage 2: *excavation of the gallery by 1-meter steps, up to reaching the Test Drift zone, with activation of the concrete lining simultaneously. The excavation speed is 2m/day*. In this second stage, the excavation of one meter large bloc of Boom Clay is modelled by desactivating the corresponding group of rock elements, and by activating at the same time the corresponding contact elements along the lining. Thus the tip of the gallery moves towards the *Test Drift* zone. The exact set of rock elements to be desactivated is determined at each step, by checking the elements which, in the present state, enter partially or totally in the 2.42 meter excavation zone. In fact, in the simulation (and in the reality too) the rock mass ahead of the excavated gallery moves both towards the gallery axis, and along the axis in Y direction (Figure 3). Then some elements which were outside of the profile of the gallery before excavation of the first N steps, may have entered this profile at the time when the step N+1 is processed. The modelling strategy defined allows to take into account this difficult effect properly. The height "excavated" numerically is at least 2.42 meters thus the soil around the excavated zone is free to converge towards the activated lining and eventually to come in contact with it. Moreover, it is interesting to note that, in the real excavation process, the profile of the excavation suffers irregularities, as the rock blocks which detach from the front under the action of the excavator do not exactly match the predefined profile.

3.4 *Initial and boundary conditions*

The clay formation around the gallery is considered as homogeneous and isotropic. The initial stresses are supposed to be hydrostatic ($\sigma_0 = \sigma_h = \sigma_v$). The stresses and pore pressure initial values used in the code are the in situ one (at depth of the gallery) (Table 1).

Table 1. Initial stress and pore pressure around the gallery.

Total isotropic stress ($\sigma_0 = \sigma_h = \sigma_v$)	4.5 MPa
Pore Pressure	2.2 MPa
Effective Stress	2.3 MPa

3.5 *Constitutive laws and hydraulic properties*

The hypoplastic law CLoE implemented in the FEM code *Lagamine* was used to describe the stress-strain relation for Boom Clay. An experimental program has been carried out in the SELFRAC project (Bernier et al. 2005) to obtain the main input parameters needed to calibrate this constitutive law.

Full saturation is assumed in this work. The main hydraulic properties used for the simulation are given in Table 3. Permeability is considered isotropic.

Table 3. Hydraulic properties for Boom Clay at a 225 meters

Water permeability	[m^2]	$3{,}5.10^{-19}$
Porosity	[%]	0.39
Water compressibility	[Pa^{-1}]	$4{,}5.10^{-10}$
Water viscosity	[Pa.s]	0.00089
Specific weight	[kg/m^3]	997

The lining is modelled using porous mechanical elements associated to an elastic constitutive law (E = 15 GPa ; ν = 0.3) . Initial stress and pore pressure in

in these elements are equal to zero. A high permeability (1.10^{-12} m^2) is chosen in order to ensure drained conditions in the lining.

4 RESULTS

In the sequel, we discuss the two main stages of the simulation : stress release around the 30 meters gallery in the initial stage, then progressive excavation of the remaining gallery.

4.1 *Stage 1: stress release in the gallery*

Illustrations in Figure 4 show the pore pressure (p_p) and the deviatoric stress (q) distribution around the gallery induced by stress release in the gallery. The rightmost picture indicates where strain localisation occurs (bifurcation criterion met locally). Note that, for sake of clarity, the lining is not represented on these pictures. More precisely, the quantities (stresses, pressures) represented in the pictures are displayed for the soil elements only, not for the lining element. As described above, at the start of the excavation process in the model, the excavation has already been performed over 30 meters and the lining is supporting the gallery up to the excavation front along these 30 meters.

The most significant perturbation occurs in a zone close to the excavation front. Pore pressure is perturbated up to 7 meters ahead the front along the axis of the gallery, and about 4 meters radially. Starting from the 2.2 MPa far field pore pressure (yellow in the picture a) we can observe a decrease down to zero and then to a significant negative pore pressure near the front (suction about -1.33 MPa). Conversely, a zone of over pressure appears near the edge of the lining, extending over about one meter along this one in the direction of the gallery. This is consistent with a over-compression of the rock locally at the contact with the lining.

Axial (σ_y) and radial stress (σ_x) are compressive everywhere, they show significant variations over about 13 meters behind the front in the axial direction, and about 10 meters in the radial direction. The increase of the radial stress just behind the front is as high as 3.5 MPa, and the axial stress increases up to 6 MPa.

Zones with potential strain localization are detected behind the front over a length of 2.5m in the axial direction. So-called “bifurcation crosses” illustrated in Figure 4 are displayed at the locations where the bifurcation criterion was found to be met. The green and the red arrows indicate the directions parallel to the two conjugate potential shear bands in this location. These two directions are rather close, which is typical of brittle materials. In the numerical model used, no post-localisation strategy has been developed. The localisation prediction displayed is indicative of zones where rupture is likely to develop in a localized mode, nothing more.

The effect of different choices in modeling the installation of the lining, on the rupture mode, has been studied by performing different simulations : in the first one, the lining was considered as instantaneously installed up to the actual position of the excavation front, while in the second there was a gap between the front and the lining along which the soil was free to move. A third computation with a finer mesh in the critical zone allowed a more precise description of the localization. It is worth to mention that no significant changes appeared between these different simulations in the pore pressure and stress fields.

4.2 *Stage 2 : excavation meter by meter up to the Test Drift zone*

The excavation was modelled according to the modelling procedure described above. Figure 5 presents the evolution of the pore pressure field in the clay during the excavation process, for a few steps arbitrary chosen between the 30 steps performed. The field is characterized by a figure of strong gradient, around the excavation front, and limited evolution of the shape of the contours from one step to the other. This observation means that the pore pressure field near the front during the excavation process is not significantly influenced by the actual position of the front; a kind of steady state is reached, which is translated with the front as the excavation progresses.

4.3 *Pore pressures changes : comparison with in situ measurements*

Results were discussed with comparison to the in situ measurement taken during the excavation. The piezometer and inclinometer transducers were placed in 8 boreholes. The position of the boreholes is summarised in Figure 6, in a radial versus axial position system.

Significant pore pressure differences between the sensors detected before the start of the excavation are out of the scope of our simulations, since they are likely to be due to previous stages in the building of the URL. Accordingly, all the sensors have the same initial pore pressure value, close to 2.2 MPa, e.g. in the different sensors response predictions presented in Figure 7.

When the excavation front is approaching the *test drift* zone, a slight increase of pore pressure is predicted but not of the order of magnitude of the actual one as measured by the real sensors (boreholes A2 and B2).

The drop of pore pressure is well predicted in borehole A2, sensors WA5, and in borehole B2, sensors WB5, and WB1 if we disregard the small peak

discussed above. Conversely, the prediction seems not good at all for the sensor, WC1 and WC8, WD1 and WD5.

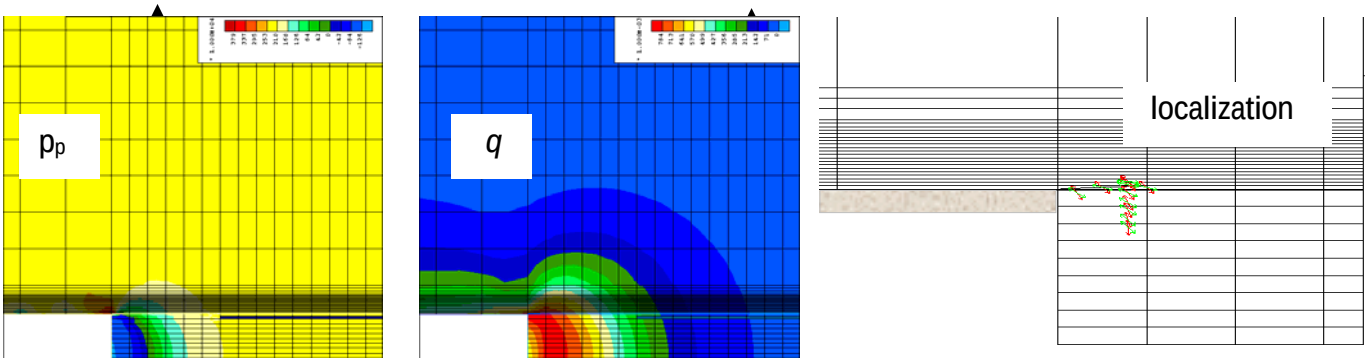

Figure 4: Stress field distribution around the 30 meter initial gallery : Pp) Stress pore pressure, q) deviatoric stress q, e) localised zones due to stress release in the gallery (bifurcation crosses located at Gauss points).

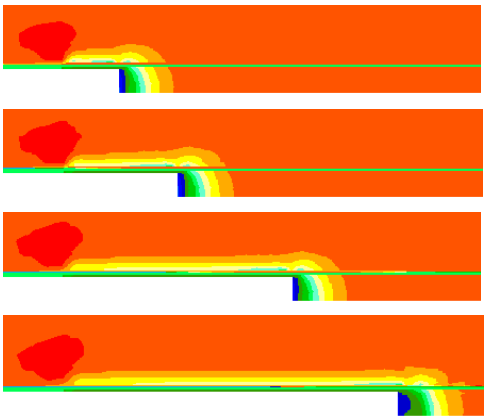

Figure 5 - Pore pressure field in the Clay at different stages of the excavation process : 5, 10, 20, 30 meters

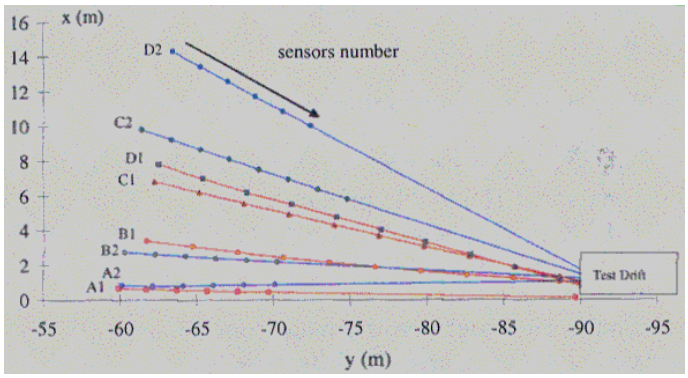

Figure 6 - location of the Clipex instrumentation boreholes in an axisymmetric system.

Concerning the latter, it should be considered that the range of variation of the pore pressure is much smaller than in the other locations, in such a way that at the same scale, the prediction seems much closer to the in-situ data. As for WA1, the discrepancy is quite significant, but the response of the sensor is different (much more abrupt) from the other evolutions observed, so there may be something special taking place there in the real process, like for example a fissure propagating from the excavation front, starting from the tip of the lining as suggested by the localisation detection presented above in Figure 4 and observed also during the excavation work.

Globally, what comes out from these comparisons is that the pore pressure drop resulting from the excavation is sensible much farer in the real world than in the simulation : A1, A5, B1, not B5; C1 and C8. Moreover, supposing that the sensors were able to measure negative pore pressure (which was not the case in fact), the negative pore pressure predicted in A1 and B5 could not be observed, because the sensors come to communicate with the gallery air pressure through fractures taking place as the front comes too close. The same comment apply to B1, because the sensor, although not destroyed by the excavation process, is very close to the lining after excavation and this is likely to induce a desaturation of the sensor after the front has passed its location, while the simulation reports a small area of excess pore pressure to pass by the sensor location and to induce the small peak observed in the WB1 curve.

4.4 *Sensitivity analysis*

In order to check the sensitivity of the results presented to some details of the modeling strategy adopted, the whole simulation has been reproduced with two significantly changed configurations: first, a different set of parameter was used for the constitutive law, corresponding to a more contractant material (determined from the higher mean effective stress experimental tests); secondly, the duration of the deconfinement of the first section of the gallery was changed from 15 days to 1 day. The results were carefully compared with the reference simulation presented here. Some changes were observed in both cases, but nothing significant.

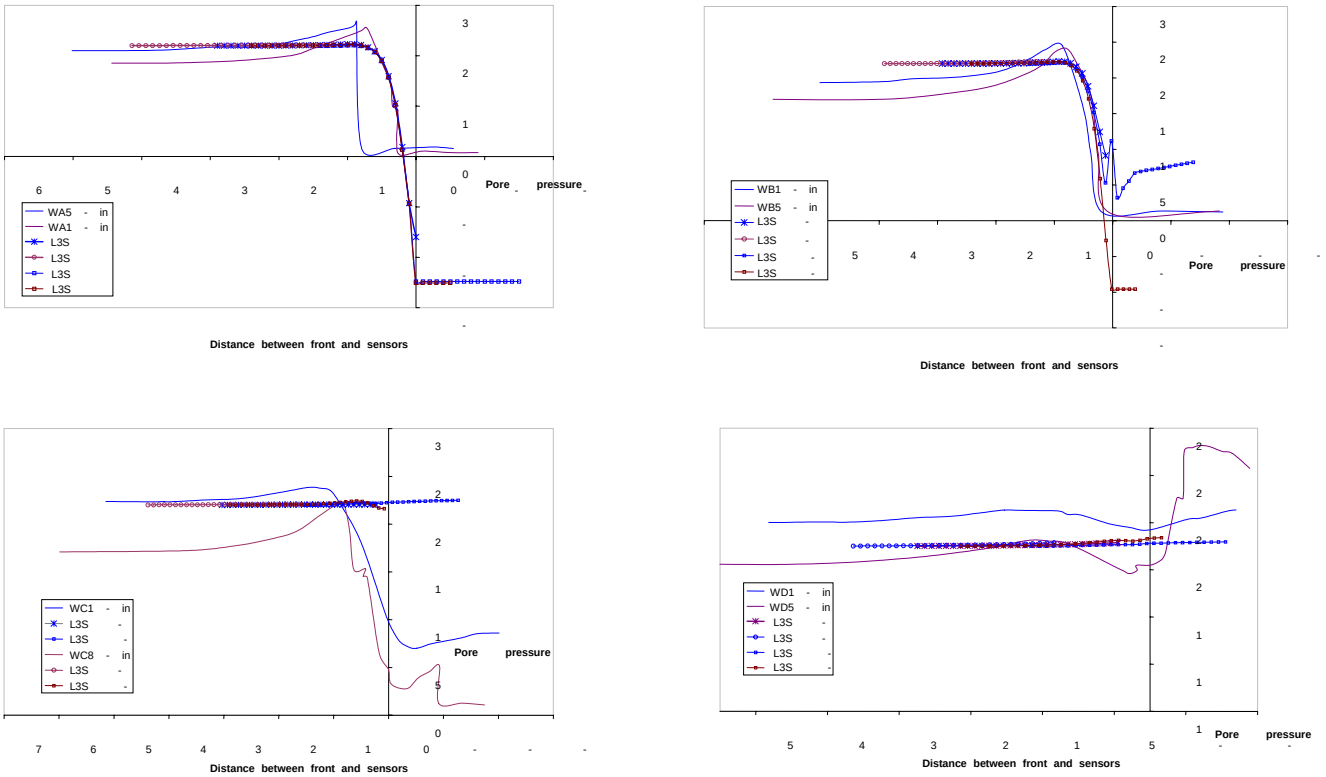

Figure 7: Pore pressure comparisons with in-situ measurements during the excavation up to the test drift zone.

5 CONCLUSIONS

The modeling of the excavation process and the strain localization prediction along the process have been performed using the finite strain Finite Element Code Lagamine, with the constitutive law CLoE. A special modeling procedure was designed, taking into account the progressive excavation as a process in time, the placement of a lining behind the excavation front, the existence of a over-excavation with respect to the lining dimensions, and the hydromechanical coupling. The results are consistent with the site observations, especially the localization predicted. Further refinements would be necessary to reduce some discrepancies observed with respect to site data.

ACKNOWLEDGEMENTS

This work was performed in a partial fulfillment of the SELFRAC contract FIKW-CT 2001-00182 co-funded by the European Community under the '5th Euratom Framework Program' (1998-2002).

REFERENCES

Bernier, F., Li, X.L., Verstricht, J., Barnichon, J.D., Labiouse, V., Bastiaens, W., Palut, J.M., Ben Slimane, K., Ghoreychi, M., Gaombalet, J., Huertas, F., Galera, J.M., Merrien, K., Elorza, F.J. & Davies, C., 2002. CLIPEX. Report EUR 20619, Luxembourg: Commission of the European Communities

F. Bernier, X.L. Li, W. Bastiaens, L. Ortiz, M. Van Geet, L. Wouters, B. Frieg, P. Blümling, J. Desrues, G. Viaggiani, C. Coll, S. Chanchole, V. De Greef, R. Hamza, L. Malinsky, A.Vervoort, Y. Vanbrabant, B. Debecker, J. Verstraelen, A. Govaerts, M. Wevers, V. Labiouse, S. Escoffier, J.-F. Mathier, L. Gastaldo, Ch. Bühler, 2005, FRACTURES AND SELF-HEALING WITHIN THE EXCAVATION DISTURBED ZONE IN CLAYS. Commission of the European Communities

Cescotto S., Charlier R. 1993 Frictional contact finite elements based on mixed variational principles, *Int. J. of Numerical Methods in Engineering*, **36**, pp 1681-1701

Chambon R., Desrues J., Charlier R., Hammad W. 1994. CLoE, a New Rate Type Constitutive Model for Geomaterials: Theoretical Basis and Implementation, *Int. J. Num. Anal. Meth. Geom.* **18** No 4, pp. 253-278

Charlier R. 1987. *Approche unifiée de quelques problèmes non linéaires de mécanique des milieux continus par la méthode des éléments finis*, Ph.D. thesis, University of Liège, Belgium

Coll C. 2005. Endommagement des Roches Argileuses et Perméabilité Induite au Voisinage d'Ouvrages Souterrains, Thèse Doctorat UJF, Grenoble, France, 257 p.

Collin F., Li X.L., Radu J.P. & Charlier R. 2002. Thermo-hydro-mechanical coupling in clay barriers, *Engineering Geology* **64**, pp. 179-193

Desrues J., Chambon R. 2002a. Shear bands Analysis and Shear Moduli Calibration, *Int. Journal Solids and Structures* **39** No 13-14, pp. 3757-3776

Desrues J., Chambon R. 2002b. Modélisation d'une Argilite à l'aide du modèle CLoE, *Revue Française de Génie Civil* **6** No 1, pp. 89-113